Science of the Total Environment 854 (2023) 158661

Contents lists available at ScienceDirect

Science of the Total Environment

journal homepage: www.elsevier.com/locate/scitotenv

Quantification and uncertainty of root growth stimulation by elevated CO_2 in a mature temperate deciduous forest

Clare Ziegler [a,b], Aleksandra Kulawska [a,c], Angeliki Kourmouli [a,c], Liz Hamilton [a,c], Zongbo Shi [a,c], A. Rob MacKenzie [a,c], Rosemary J. Dyson [a,d], Iain G. Johnston [e,f,a,*]

[a] Birmingham Institute of Forest Research, University of Birmingham, Birmingham, UK
[b] School of Biosciences, University of Birmingham, Birmingham, UK
[c] School of Geography, Earth and Environmental Sciences, University of Birmingham, Birmingham, UK
[d] School of Mathematics, University of Birmingham, Birmingham, UK
[e] Department of Mathematics, University of Bergen, Bergen, Norway
[f] Computational Biology Unit, University of Bergen, Bergen, Norway

HIGHLIGHTS

- Faster fine root production and higher belowground NPP under elevated CO_2.
- Stochastic modelling shows less bounded root growth in eCO_2 than control.
- Both elongation and thickening of fine roots under eCO_2 contribute.
- Uncertainty quantified in multifaceted estimates of belowground NPP.

GRAPHICAL ABSTRACT

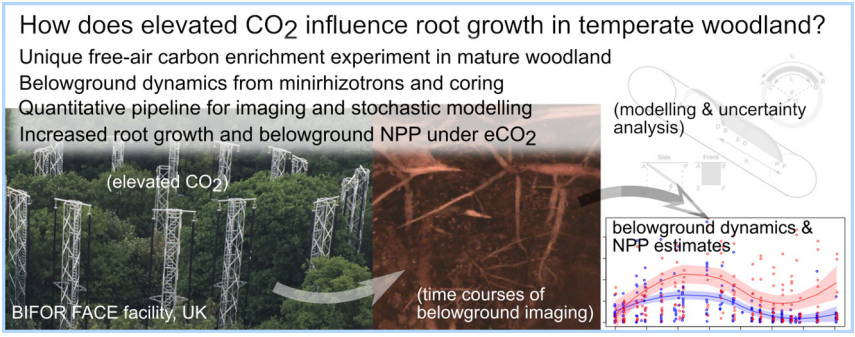

ARTICLE INFO

Editor: Elena Paoletti

Keywords:
Elevated CO_2
Belowground NPP
Fine roots
Mature temperate woodland
Mathematical modelling

ABSTRACT

Increasing CO_2 levels are a major global challenge, and the potential mitigation of anthropogenic CO_2 emissions by natural carbon sinks remains poorly understood. The uptake of elevated CO_2 (eCO_2) by the terrestrial biosphere, and subsequent sequestration as biomass in ecosystems, remain hard to quantify in natural ecosystems. Here, we combine field observations of fine root stocks and flows, derived from belowground imaging and soil cores, with image analysis, stochastic modelling, and statistical inference, to elucidate belowground root dynamics in a mature temperate deciduous forest under free-air eCO_2 to 150 ppm above ambient levels. eCO_2 led to relatively faster root production (a peak volume fold change of 4.52 ± 0.44 eCO_2 versus 2.58 ± 0.21 control), with increased root elongation relative to decay the likely causal mechanism for this acceleration. Physical analysis of 552 root systems from soil cores support this picture, with lengths and widths of fine roots significantly increasing under eCO_2. Estimated fine root contributions to belowground net primary productivity increase under eCO_2 (mean annual 204 ± 93 g dw m^{-2} yr^{-1} eCO_2 versus 140 ± 60 g dw m^{-2} yr^{-1} control). This multi-faceted approach thus sheds quantitative light on the challenging characterisation of the eCO_2 response of root biomass in mature temperate forests.

1. Introduction

Human-induced carbon dioxide (CO_2) emissions are a major contributor to climate change, making up the majority of anthropogenic greenhouse gas emissions (Quere et al., 2018). Rising atmospheric levels of CO_2 due to

* Corresponding author at: Department of Mathematics, University of Bergen, Bergen, Norway.
E-mail address: iain.johnston@uib.no (I.G. Johnston).

http://dx.doi.org/10.1016/j.scitotenv.2022.158661
Received 26 July 2022; Received in revised form 5 September 2022; Accepted 6 September 2022
Available online 9 September 2022

anthropogenic emissions are partly mitigated by terrestrial and marine carbon sinks which take up CO_2. However, the behaviour of land-based carbon sinks as CO_2 levels continue to increase remains poorly understood, challenging both our fundamental scientific understanding and our ability to plan strategies to combat CO_2 increases (Masson-Delmotte et al., 2018; Terrer et al., 2019).

The world's forests are major actors in the global carbon budget (Pan et al., 2011), and it is important to understand the effects of increased CO_2 on these ecosystems in order to make wider climate change predictions (Bradley and Pregitzer, 2007; Pugh et al., 2016; Medlyn et al., 2015). This in turn necessitates an understanding of the effect of increased carbon on plant growth and dynamics (Cleland et al., 2007). Aboveground processes such as photosynthesis, although logistically challenging to analyse in mature forest systems, are amenable to *in situ* measurements and remote sensing. However, belowground processes are harder to measure and less frequently studied, so constitute a substantial source of uncertainty in our knowledge of the carbon budget. The production of belowground fine roots is an important player in the global carbon budget (Clemmensen et al., 2013), suggested to be responsible for up to 33 % of global NPP (Jackson et al., 1997; Gill and Jackson, 2000), and up to a third of C and N mineralised in temperate forest soils (Finzi et al., 2015).

Carbon fertilisation, where elevated CO_2 (eCO_2) leads to increased biomass production, may lead to belowground root mass being an increasingly important carbon sink in a high-CO_2 world. Increasing root mass in growing forests, and stocks and flows in mature forests pushed out of equilibrium by eCO_2, both contribute to this sink. However, increased growth under elevated CO_2 leads to a greater dependence on soil nutrient availability (Norby et al., 2010; Norby et al., 2016; Zaehle et al., 2014) (particularly noted in agricultural studies due to decreased nutritional value in crops (Myers et al., 2014; Fernando et al., 2014)). Nitrogen and phosphate availability appears to be of particular importance in long-term growth response (Cavagnaro et al., 2011; Ellsworth et al., 2017; Terrer et al., 2019), and may become a limiting factor in non-fertilised soils. Tight coupling between nitrogen levels and phosphate mobility in soils (Marklein and Houlton, 2012) may also lead to root growth becoming phosphate limited (Edwards et al., 2006). Due to such nutrient limitations, the capacity for carbon fertilisation of fine root growth may thus be limited both in magnitude and duration, possibly limiting its long term potential as a carbon sink (Terrer et al., 2019; Norby and Zak, 2011). Belowground colonisation via root system expansion may allow plants to overcome some nutrient limitation effects, as additional nutrients may be accessed. Such colonisation in mature ecosytems may be limited by competition for space; hyphae of mycorrhizal fungi can contribute by accessing regions inaccessible to roots, and these microbial communities remain relatively stable with eCO_2 (Norby and Zak, 2011). Generally, the difficulties of non-destructive observation of below-ground systems (Felipe-Lucia et al., 2018) mean that the extent and timescale of carbon fertilisation of belowground root mass remains challenging to quantify, particularly in mature forests. Observations are often obtained using destructive sampling, or using minirhizotrons (see below) to image belowground root systems. The use of such samples (taken from a limited, geometrically non-trivial, and uncertain volume of the belowground system) to estimate system-wide properties creates substantial uncertainty that is itself challenging to quantify (Norby et al., 2004; Tierney and Fahey, 2001; Majdi, 1996; Taylor et al., 2014).

Previous experiments have characterised the effect of eCO_2 on specific root systems (Matamala et al., 2003; Bader et al., 2009), finding that carbon enrichment influences (and often enhances) fine root growth and increases elemental uptake through fine roots (Bader et al., 2009; Jiang et al., 2020; Norby et al., 2004; Iversen, 2010; Iversen et al., 2008; Pritchard et al., 2008; Pepin and Korner, 2002) although data remain sparse. There is a general consensus that eCO_2 leads to an initial increase in carbon capture and growth in both above-ground (Norby et al., 2002; Thilakarathne et al., 2015) and below-ground tissues (Allen et al., 2000) (including in our experimental site described below (Gardner et al., 2022)). Recent experiments in mature forest have shown that initially increased primary production due to eCO_2 does not necessarily lead to increased carbon sequestration, as respiration releases the additional carbon back to the atmosphere (Jiang et al., 2020). Growth increases may be limited by nutrient availability (Johnson et al., 2004; Reich et al., 2014; Rogers et al., 1999), with many short-term experiments failing to capture this effect (Madhu and Hatfield, 2013) which may only be visible in experiments run over many years (Norby et al., 2010). Contributions to the experimental and theoretical challenges in the field include the twin logistic difficulties of elevating CO_2 in a natural ecosystem (Terrer et al., 2019; Norby and Zak, 2011) and performing repeated non-invasive belowground measurements therein, the heterogeneity of natural belowground root systems, and the natural variability in root dynamics.

Here, we address these difficulties with an interdisciplinary workflow, coupling free air CO_2 enrichment (FACE) experiments (Hart et al., 2019; Nowak et al., 2004; Oak Ridge National Laboratory, n.d.; Lapola and Norby, 2014; U.S. Department of Energy, 2020) (see also meta-study in Terrer et al. (2019) and commentary in Norby and Zak (2011)) in a natural ecosystem, large-scale belowground imaging with minirhizotrons in parallel with destructive soil coring, a semi-automated image analysis pipeline, and novel applications of mathematical tools from stochastic processes and statistical inference. We work in a native, mature, deciduous UK woodland (Hart et al., 2019). Temperate land ecosystems at these latitudes constitute the joint highest (with equatorial land ecosystems) source of climate model uncertainty in carbon-cycle feedbacks (Ciais and Sabine, 2013). Our overarching hypothesis was that eCO_2 would enhance fine root growth and belowground productivity in this system, but that this enhancement would be potentially limited by the fact that some belowground space was already colonised in this mature ecosystem. We therefore hypothesized that this carbon fertilisation would involve a combination of new root exploration and existing root expansion, and, as a parallel methodological hypothesis, that modelling approaches would help dissect the various sources of uncertainty in these challenging observations.

2. Material and methods

2.1. Experimental site

Our field observations were carried out at the Birmingham Institute of Forest Research (BIFoR) FACE facility (Hart et al., 2019) in the UK (Fig. 1A). The BIFoR FACE site was chosen as typical of under-managed temperate broadleaf forest close to the University of Birmingham. The soil was characterised ahead of the establishment of the FACE patches and the root minirhizotron sites (see below). The BIFOR FACE facility has been built into a native mature deciduous woodland, dominated by oak (*Quercus robur*) interspersed with hazel (*Corylus avellana*) coppice. Sycamore (*Acer pseudplatanus*), hawthorn (*Crataegus monogyna*) and holly (*Ilex aquifolium*) have self-seeded into gaps and, with the hazel, form a distinct sub-canopy. The forest grows on centuries-old Orthic Luvisol soil with a mul-moder humus classification (Hart et al., 2019; Iuss Working Group Wrb, 2015); more details on soil and uniformity across the site can be found in MacKenzie et al. (2021b). The experimental design consists of three eCO_2 and three ambient-air control regions (as in the Australian EucFACE study (Duursma et al., 2016)). These regions, which we refer to as arrays, are 30 m diameter rings, with free-standing towers extending above the ~25 m oak canopy (Fig. 1B). Pipes attached to the towers emit treated air with increased CO_2, in order to raise the CO_2 levels within the eCO_2 arrays to 150 ppm above the ambient (calculated as the lowest CO_2 mixing ratio measured in the control arrays). A CO_2 elevation of 150 ppm was chosen to ensure that results are relevant to policy, representing mid-21st-century planetary-average mixing ratios. Under most shared socioeconomic pathways and reactive concentration pathways, atmospheric CO_2 is expected to peak at or exceed the +150 ppm treatment (Cheng et al., 2022). The control arrays are identical, but the air released into the array contains no additional CO_2. Performance of the facility was excellent over the course of these experiments, with details and further information available in Refs. (Gardner et al., 2022; Hart et al., 2019; MacKenzie et al., 2021a).

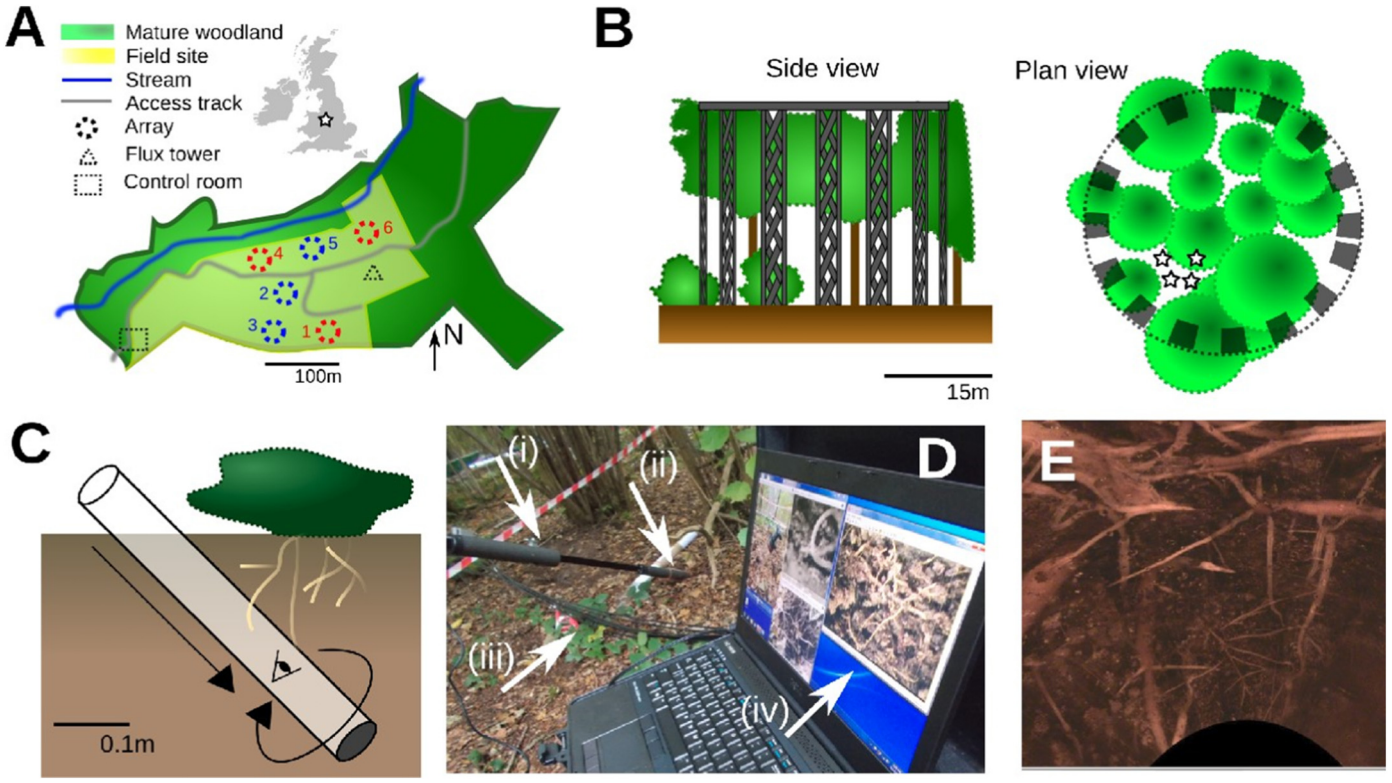

Fig. 1. Field experiments tracking root dynamics under control and eCO_2 conditions. (A) The BIFoR FACE experimental facility is situated in mature deciduous woodland near Stafford, UK, and contains three eCO_2 (red) and three control (blue) 'arrays'. (B) Arrays consist of scaffolding (grey) supporting pipes carrying eCO_2 or ambient air to the forest canopy. Each array has four minirhizotron installation sites. (A-B) adapted from Ref. (Hart et al., 2019). (C) Minirhizotron sites consist of a transparent tube embedded at a 45° angle in the soil, covered and sealed when not in use. (D) A camera and lighting system (i) is inserted into each of these tubes (ii) to take belowground images of in situ root systems around the tube circumference and along its length. The imaging system is connected (iii) to a field power supply and to a computer running real-time image acquisition software (iv). (E) Illustration of data acquired from minirhizotrons; this composite consists of many images concatenated and embedded on a cylindrical manifold for illustrative purposes.

No substantial changes in the floral community composition was observed during, or since, the eCO_2 treatment patches described here.

BIFoR FACE, situated in a mixed woodland, involves studying plants within a diverse preexisting ecosystem rather than a plantation as with many previous FACE experiments (Norton et al., 2008; Hendrey et al., 1999). Therefore, data collection methods need to be as non-destructive as possible. Minirhizotrons (see Section 2.2) allow a small subset of a root system to be observed over time (Johnson et al., 2001), but can by nature obstruct the natural structure of the root system, and require indirect biomass quantification (Taylor et al., 1990). Soil cores are a more destructive sampling method and do not allow long-timescale observation of the same region, but allow for more direct estimations of root biomass and turnover (Samson and Sinclair, 1994). Both methods have been successfully employed in previous studies of fine root growth (Iversen, 2010). Here, we use a workflow coupling the two modes of investigation (see Discussion) with new theoretical developments and a rigorous treatment of uncertainty (Johnston et al., 2014) to maximise the interpretability and transferrability of our results. The observations described below were taken over a two-year time period, forming the first set of field observations from this experiment.

2.2. Minirhizotron installation

Four 50 cm long minirhizotron tubes sealed with bungs (custom machined at University of Birmingham) were installed in each array, with the sites chosen to keep the species makeup of surrounding vegetation as consistent as possible. A Van Walt (Prestwick Lane, Surrey, GU27 2DU) 55 mm corer was used to remove a cylinder of soil at a 45° angle. The minirhizotron tube, sealed at the lower end and with a removable bung at the upper end, was then inserted manually into the hole, with care taken to prevent damage to the exterior of the tube. Each set of four was installed in a designated area within the array with clear markers to minimise footfall. The tubes were then numbered 1–4 for ease of referencing. Four 50 cm tubes were installed in each of the 6 control and eCO_2 arrays, leading to 24 tubes in total. Data was also collected from two 2 m tubes previously installed in Arrays 1 and 6. A further 50 cm tube was later installed at the entrance of Array 2 for demonstrational purposes (Fig. 1D). The limited aboveground section of the tube was covered when not in use. Installation took place from 28/11/2016 to 8/12/2016, leaving 4 months for the system to equilibrate before experiments began (Johnson et al., 2001).

2.3. Total root imaging and physical characterisation

A Bartz Technology Corporation (VSI Bartz Technology Corporation 4187 Carpinteria Ave Unit #7. Carpinteria Ca. 93013 USA) 100× minirhizotron camera system (Johnson and Meyer, 1998) with Smucker manual indexing handle (Ferguson and Smucker, 1989) was used to obtain the root images, and paired with a Bartz Technology Corporation I-CAP image capture system. The bung was carefully removed from the end of the tube, with one hand stabilising the tube during removal, and the camera was then inserted. The tubes were scanned for roots, starting from the bottom and working up. Roots are photographed and the depth, viewing angle from vertical, and tube number are recorded. The images are then analysed using SmartRoot (Lobet et al., 2011) as described below, and the amount of new growth and branching is recorded through comparison with earlier images. Data was collected monthly, from all tubes in all arrays. Smart Root measurements were calibrated to cm, and, where required, volume measurements were converted to dry weight biomass using a conversion factor

of 343 mg dw cm^{-3}, obtained from a comparison of root masses from soil cores and scans of the same samples analysed with SmartRoot (see below).

2.4. Image analysis

Image analysis (see Fig. S1) was performed using SmartRoot (Lobet et al., 2011), a plugin for ImageJ (Schneider et al., 2012) which we used as part of the Fiji package (Schindelin et al., 2012). Roots were manually identified using the software, and a skeleton was produced with periodic width measurements along the root. The length of each root segment was recorded along with an average width across each width measurement point. Each segment was recorded with a length and width measurement in cm, along with the array number, tube number, date of sampling, depth of sampling as taken from the Smucker manual indexing handle, and angle of measurement when available. The image analysis was performed by a single person so that any subjectivity in root identification would remain constant across eCO_2 and control populations.

2.5. Soil coring

Soil cores were taken periodically over the two year study period; in March 2017, March, July, November of 2018, and March 2019. Three cores of length 30 cm and diameter 5 cm were taken from each array at BIFoR using a lined Van Walt 55 mm corer. The cores were separated by horizon (visually identified by soil colour and texture) and the roots were hand-picked from each sample, and live and dead roots were separated. Live roots were identified based on the criteria in (Santantonio and Hermann, 1985), with preliminary experiments to confirm this protocol using Evans Blue vital stain (Sigma Aldrich). Roots were then washed, dried, and the mass recorded for each sample.

2.6. Root scans from soil cores

We manually recorded the length and diameter of 552 root systems (3709 roots in total) recovered from soil cores taken in March 2019. After separation and washing roots as above, roots <2 mm thick were blotted to remove excess water and carefully teased apart using forceps to display as much of the natural root system as possible while minimising breakages. Roots were removed from water then carefully laid out on a scanner, with as much separation as possible to aid in later image analysis (see Fig. 4A). 1 cm graph paper was used as the backing to allow easy scaling of the image. The scanner lid was closed carefully to minimise movement of roots, and cleaned with a paper towel between scans to remove any debris. Each root was manually traced and automatically measured with SmartRoot.

2.7. Statistical analysis and uncertainty quantification

Statistical analysis was performed in R (Team, 2015) using custom scripts available at github.com/stochasticbiology/elevated-co2. We used LOESS fitting for exploratory analysis of the time series data. LOESS (locally estimated scatterplot smoothing) is an approach for summarising noisy scattered data, which is non-parameteric – and hence does not rely on specific assumptions about the distributions from which observations are drawn or the form of the time behaviour of the data (assumptions that would be needed in, for example, ANOVA and *t*-test approaches). LOESS fitting was performed using the default parameterisation of the *loess* command, specifically using a span α of 0.75 and a polynomial degree of 2.

LOESS does not admit straightforward hypothesis testing, so we used alternative approaches for testing specific hypotheses. Again, to avoid assumptions about the distributions from which our observations were drawn, we the non-parametric Mann-Whitney test for comparing medians of observation sets. This approach avoids making assumptions about the normality of observations.

Caladis (Johnston et al., 2014) was used for uncertainty propagation, specifically to track uncertainty through the calculation of Eq. (4). Caladis is an online tool allowing for calculations using probability distributions (Johnston et al., 2014). Each variable in a calculation is associated with a user-defined probability distribution reflecting uncertainty in that quantity, and when a calculation is performed the value of each variable is sampled from its distribution for use in the equation. In the Supplementary Information we detail and justify the uncertainty distributions used in our NPP calculation.

2.8. Raw data

All raw data (and analysis code) are available at https://github.com/stochasticbiology/elevated-co2

3. Theory and calculation

3.1. Birth-immigration-death model dynamics

A birth-immigration-death (BID) stochastic model can be applied to root system data by considering a unit length of root as a member of the root 'population'. Here, the observed system is the fine root volume in our experiments, and the mechanisms we consider are growth of existing roots, new roots entering the field of observation (the viewing region of a minirhizotron) and disappearance of existing roots. These mechanisms have well-studied analogues in stochastic processes: so-called birth (the replication of existing elements), immigration (the arrival of new elements from outside the system) and death (the removal of existing elements). We therefore work in a birth-immigration-death (BID) modelling framework Methods. The task is, given observations of fine root volume, to infer the rates of birth, immigration, and death in eCO_2 and control experiments. We proceed by obtaining the likelihood function associated with the BID model, which describes the probability of seeing a given amount of root volume at a given time when the rate parameters take given values. The parameter values that maximise this likelihood function for our data then correspond to the most likely rates for the three processes.

We will use E and V to refer to the expected value and variance of a random variable respectively. Taking m as the number of unit root lengths, λm the birth rate, νm the death rate and α the immigration rate, this model is described by the master equation

$$\frac{dP_m}{dt} = (\alpha + \lambda(m-1))P_{m-1} + \upsilon\,(m+1)P_{m+1} - (\alpha + \lambda m + \upsilon m)P_m \quad (1)$$

for $P_m(t)$, the probability of a state with m unit root elements at time t. Initial conditions at $t = 0$, $\mathrm{E}(m, t = 0) = m_0$ and $\mathrm{V}(m, t = 0) = v_0$, are also parameters of the model. The BID model admits a closed-form solution for an exact likelihood (which has been previously studied in stochastic biology (Johnston and Jones, 2015)), but for simplicity and because of the continuous nature of our root observations we employ a normal approximation. Hence, we set the probability of an observation m at time t' to be normally distributed:

$$P(m, t') = N(E(m, t'), V(m, t')) \quad (2)$$

using expressions for E(*m, t'*) and V(*m, t'*), the mean and variance of root biomass observed at time *t'*, which we derive in the Supplementary Information.

This approach has several strengths in the analysis of data like ours. First, the distributional detail of observations is captured, so that scientific information can be gained from the variance of observations as well as their mean trends, accounting for possible nonzero initial variance due to measurement noise. Second, the approach is naturally dynamic, allowing time series data to be naturally analysed, with more time points providing more statistical power. Third, the BID model supports both stable and exponentially varying solutions, allowing transient as well as longer-term effects to be learned from the data. This third point, in separately accounting for initial and ongoing behaviour, mitigates against the high weighting of initial observations in the fold-change calculation above.

3.2. Fine root production for NPP calculation

Fine root production was calculated by observing growth of specific root branches in the top strip of a tube in each of the six arrays (Norby et al., 2004; Tierney and Fahey, 2001; Majdi, 1996). The roots were observed monthly as described above, and the growth since the month before was recorded. This allowed the calculation of total fine root production in the viewing areas for treatment and control for each of the two years of sampling. These numbers were then scaled to give a total NPP for the arrays using the geometry of the minirhizotron installations.

In the Supplementary Information we show that the minirhizotron tube samples a proportion of the total volume of the soil column in which it is embedded:

$$V = \frac{V_s}{V_l} = \frac{l_l d(d+2r)}{2\,h\,r\,(r+d)\,\sin 2\phi} \tag{3}$$

where h is the length of the viewing area, r is the radius of the minirhizotron tube, d is depth of viewing field, ϕ is the angle of the minirhizotron tube, and l_l is the viewing arc length (calculated in the Supplementary Information). We further show that, given observed volume production p_{obs} through this sampling, the total NPP estimate is given by:

$$NPP = \frac{p_{obs}\rho}{VA} \tag{4}$$

where ρ is root density, A is the area on the surface covered by the viewing area (see Supplementary Information), and V is calculated using Eq. (3) above, giving overall:

$$NPP = \frac{2p_{obs}\rho hr(r+d)\,\sin 2\phi}{l_l d(d+2r)hw\,\cos\,\phi} \tag{5}$$

where $p_{obs}\rho$, observed volume increase multiplied by estimate root density, is the ORP observed through minirhizotron samples (see Methods), w the width of the viewing area, and ϕ is the angle of the minirhizotron tube.

4. Results

4.1. Fine root structure observed with minirhizotrons

We used minirhizotrons (Fig. 1C; see Methods) to observe belowground root systems (Fig. 1C-E; Fig. S1) in control and eCO_2 plots across a two-year time frame. 216 eCO_2 and 216 control measurements were taken, each involving around 150 individual frames of belowground imaging, for a total 6.7×10^4 frames of observed root volumes. To facilitate working with this data volume, we designed and used a semi-automated image analysis pipeline (see Methods) to quantify observed root dry weight biomass. The root volume data showed a pronounced seasonal trend (Fig. 2A), with both eCO_2 and control volume increasing from April to October 2017, then decreasing until June 2018 before increasing again through the late summer. In addition to general seasonal variation, these trends likely also include some system-specific influences (see Discussion).

At the start of the experiment (before any eCO_2 treatment) the average standing root volume in control arrays was higher than in treatment arrays. This initial difference – due to heterogeneity in the ecosystem – means that absolute magnitudes of observed volume are of less interest than the rates of change after the experiment began. Following commencement of treatment, the rates of increase of volume in spring-summer 2017 (and late summer 2018) appeared higher for eCO_2 than for control. To investigate this further, we calculated the fold-change increase in volume from the initial measurement for eCO_2 and control observations (Fig. 2B) and observed dramatically higher rates of increase for eCO_2 observations. LOESS fitting showed a maximum mean fold-change increase of 2.58 ± 0.21 for control plots and 4.53 ± 0.44 (standard errors) for eCO_2 plots. LOESS confidence intervals cannot be directly subjected to hypothesis testing, but individual observations statistically support this difference: for example, comparing fold-change observations from 150 to 300 days into the experiment gives 4.59 ± 0.58 for eCO_2 and 2.50 ± 0.31 for control (standard errors), with $p = 0.016$ from the Mann-Whitney test.

Although suggestive of a treatment effect, these fold-change measurements must be interpreted with caution as they assign more statistical weight to the initial volume measurements, which provide a reference for the subsequent scaling. To explore these trends further, we employed a stochastic model for the belowground processes influencing fine root volume. Such a mechanistic model allows us to account for time behaviour and initial conditions in a way that would be challenging using statistical treatments based on linear modelling or ANOVA-like approaches.

4.2. Stochastic modelling for fine root volume

Noting that Fig. 2A shows the strongest dynamic differences between eCO_2 and control experiments in the first 300 days, we first analysed our observations from this time window using a stochastic birth-immigration-death (BID) model (see Methods). We found that the parameters inferred to describe fine root dynamics differed significantly between eCO_2 and control experiments in the first year (likelihood ratio test, $p < 10^{-15}$). The maximum likelihood parameterisation for control experiments supported dynamics that reached a volume steady-state, while the maximum likelihood parameterisation for eCO_2 experiments supported an exponential increase over this period (Fig. 2C-D). The likelihood ratio test supporting the distinction between eCO_2 and control experiments is relative to an amalgamated model with less support (Fig. 2E). This picture is supported by the maximum likelihood value of $\lambda - \nu$, the difference between birth and death rates, which is positive ($0.0045\ day^{-1}$) for eCO_2 experiments and negative ($-0.0086\ day^{-1}$) for control experiments. Bootstrapping with the percentile method confirmed this difference ($p = 0.041$, Fig. 2F).

The BID model applied to the second year showed no statistical support for a model where eCO_2 and control root dynamics differed (likelihood ratio test), with limited differences in inferred parameters (Supplementary Fig. S2). As described above, root growth in other time periods was lower, potentially due to environmental factors. This absence of significant differences of course cannot be interpreted as a significant absence of a difference, and perhaps the more likely explanation is that absolute growth in this period was too low for differences to be detected (see below and Discussion).

4.3. Sampled root biomass and morphology from soil cores

In addition to minirhizotron measurements, we obtained periodic soil cores from the experimental plots and assessed the live and dead biomass in O (organic), A (mineral), and B (subsoil) horizons in these cores (see Methods). The specific depths of these horizons differed across the field site – we found little evidence for systematic differences between horizons in live or dead biomass from soil cores (Fig. 3A-B), including across horizons (Fig. 3C).

To explore the system further, we manually recorded the length and diameter of fine roots (<2 mm, see Methods) from 552 root systems (3709 roots in total) recovered from soil cores taken in March 2019 (Fig. 4). When treating each root sample as an independent observation, we found a low magnitude, but statistically robust, increase in root width in eCO_2 versus control (mean eCO_2 2.89×10^{-2} cm, mean control 2.79×10^{-2} cm, 1.04-fold increase), Fig. 4C). A similar signal was found in estimates of lateral root length (Supplementary Fig. S3), although these length estimates should be interpreted with some caution (see Supplementary Information). Additionally, as these root samples come from physically proximal locations in the experimental site, their treatment as independent samples is not completely accurate. Quantifying the extent of pseudo-replication from this physical colocalisation is challenging, so we instead explored the robustness of these findings with a subsampling approach. Here, we subsampled different proportions of the full observation set, effectively treating only a certain fraction of the observations as statistically independent. When only 20 % of the data were retained by subsampling, the

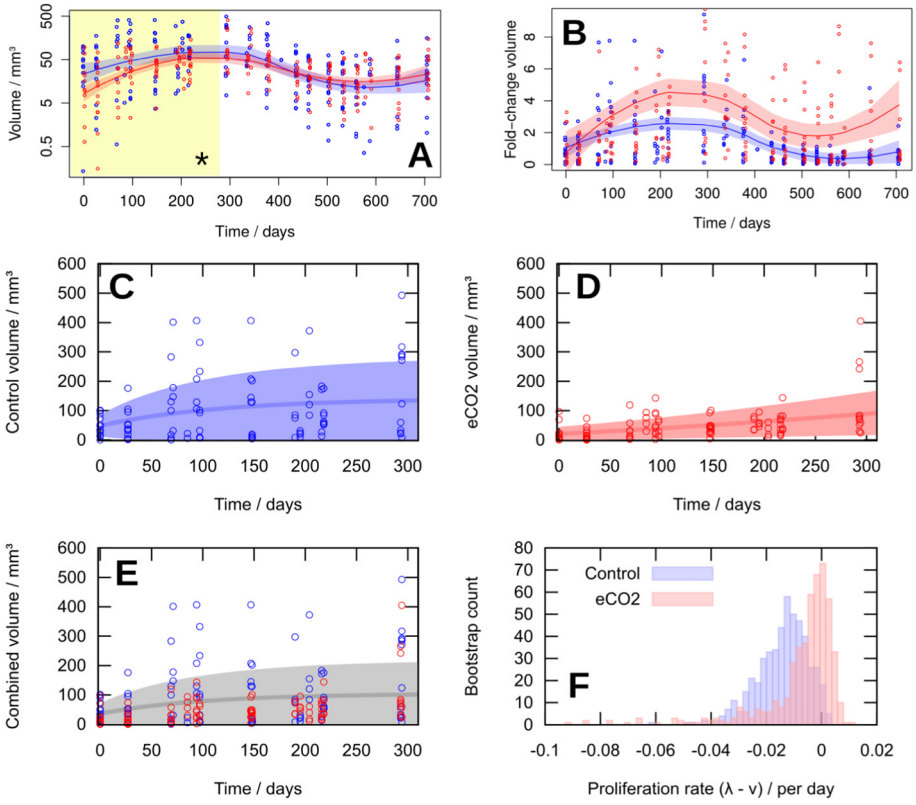

Fig. 2. Root volume changes over time under eCO_2 and control conditions. (A) Fine root volume observations in eCO_2 (red) and control (blue) experiments. Each datapoint is an observation from a single minirhizotron site. LOESS fits to the log-transformed data are shown with 95 % confidence intervals, displaying the different rates in the first 300-day period (∗, highlighted). (B) Fold change in fine root volume from initial observations. Each datapoint is an observation from a single minirhizotron site, normalised by the initial volume averaged across all sites in an individual array. (C-E) The birth-immigration-death (BID) model described in the text, applied to the first year of (C) control, (D) eCO_2, and (E) combined volume observations. Time axis gives days from 11 April 2017. The maximum likelihood BID parameterisation is found for each dataset, then the mean and standard deviation of the model for that parameterisation is plotted. A likelihood ratio test shows statistical support for the individual models (C) + (D) over the combined model (E) ($p < 10^{-15}$), indicating a difference between eCO_2 and control dynamics. (F) Bootstrapped estimates for the difference between root elongation (birth, λ) and root decay (death, ν) parameters for eCO_2 and control data. $\lambda - \nu$ is higher (with positive maximum likelihood estimate) for eCO_2, reflecting increasing root proliferation, and lower (with negative maximum likelihood estimate) for control, reflecting decreasing proliferation. Data points are measurements from individual minirhiztoron tubes.

Mann-Whitney test still gave consistent *p*-values with mean 0.04, showing that the assumption of independence can be substantially relaxed without losing the ability to detect a difference in behaviour. Taken together, these results suggest a detectable but slight increase in elongation and thickening of fine roots after two years under eCO_2.

4.4. Net primary productivity estimation and uncertainty

We next sought to estimate the contribution of root production to net primary productivity from belowground root dynamics. To this end, we follow an established method involving time-separated measurements of the same element of a root system along the top strip of the rhizotron viewing window (Norby et al., 2004; Tierney and Fahey, 2001; Majdi, 1996; Taylor et al., 2014). Here, individual roots are identified over several monthly observations, and their dynamics are tracked over this time window (Fig. 5A). We first characterised the increase in observed root production (ORP, the estimated increase of root biomass seen over time via minirhizotrons) in our system, before attempting to map this quantity to a readout of belowground NPP. To calculate ORP, we multiplied observed increases in root volume p_{obs} by estimated root density ρ (mass per unit volume), to estimate a biomass. Joint mass and volume measurements of sampled roots from soil cores (see Methods) yielded a mean density estimate of $\rho = 0.34 \pm 0.16$ g dw cm^{-3}.

We found that ORP varied substantially between arrays (Fig. 5B) but that some trends were detectable over time. First, early ORP measurements – the first six months after the experiment started – were rather higher than later measurements in both control and eCO_2 cases. This is likely an out-of-equilibrium effect due to fine roots growing back into the field of observation of the minirhizotrons. Secondly, after these transient high values decreased, the ORP dynamics in control and eCO_2 cases differed in quarters 5–8, with eCO_2 ORP starting lower, increasing to a higher peak, and decreasing to a lower trough than control. This observation was supported statistically by fitting a quadratic model to the control and treatment data in both years. No significant differences were found in year 1, but in year 2 a likelihood ratio test shows significant ($p = 2.6 \times 10^{-4}$) support for a model where control and treatment dynamics differ (with different curvatures) over a combined model where the dynamics are the same (Fig. 5B).

To connect this ORP behaviour with a belowground NPP estimate, we calculated how minirhizotron observations can be scaled to area-wide productivity estimates, while tracking uncertainty in the numerous quantities involved in this calculation. Based on the geometry of our observational setup, we derived an equation (Eq. (5)) mapping the productivity observed in the part-cylindrical viewing region of the minirhizotron tube to the corresponding surrounding volume of the soil column, and mapping this volume to the corresponding 2D surface area for interpretation as a traditional NPP measurement. Without considering uncertainty (see below), the geometric aspects of Eq. (5) provide an approximate multiplicative scaling of $\sim 5.54 \times 10^4$ for mapping ORP in g dw yr^{-1} to NPP in g dw m^{-2} yr^{-1}.

Each parameter in Eq. (5) has substantial associated uncertainty. To improve the interpretability of our belowground NPP estimate, we used

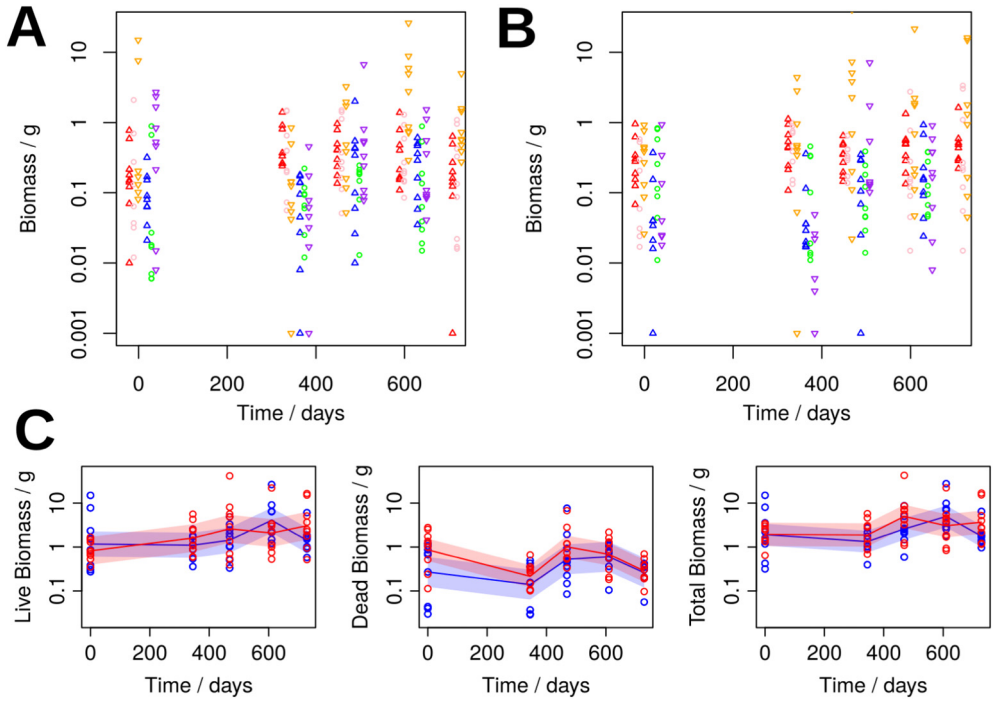

Fig. 3. No substantial differences in root biomass sampled from soil cores. (A-B) Biomass measurements from individual soil cores of 5 cm diameter separated by soil horizon for (A) control and (B) eCO_2 experiments. Time axis gives days from 11/04/2017. Horizons are O (up arrows), A (circles), B (down arrows); biomass is living (warm colours) and dead (cool colours). Data points are measurements from individual soil cores. (C) Biomass summed over all soil horizons for eCO_2 (red) and control (blue) experiments, classified by living, dead, and total. Each datapoint corresponds to a sum over the $n = 9$ cores of 5 cm diameter from a single array. LOESS fits with 95 % confidence intervals are shown.

Caladis (Johnston et al., 2014), a tool for uncertainty tracking and quantification, to propagate these uncertainties through the calculation and hence characterise the uncertainty in the final output. Expanding upon traditional uncertainty propagation, Caladis estimates full distributions over a quantity of interest given distributions over uncertain contributory factors.

Following the trends in Figs. 2–4, estimated belowground NPP was higher under eCO_2 in both years, albeit with large uncertainty when annual summaries are used. Specifically, estimated mean belowground NPP values in year 1 were 467 ± 372 g dw m^{-2} yr^{-1} for control and 551 ± 290 g dw m^{-2} yr^{-1} for eCO_2 (1.17-fold higher mean with eCO_2), and in year 2 – where transient behaviour plays a less pronounced role – were 140 ± 60 g dw m^{-2} yr^{-1} for control and 204 ± 93 g dw m^{-2} yr^{-1} for eCO_2 (1.45-fold higher mean with eCO_2) (Fig. 5B inset). The mapping from ORP to NPP substantially increases the uncertainty on these results: the distributions associated with the overall estimates are shown in Fig. 5C. This approach to calculating NPP thus characterises the very substantial uncertainty involved in estimating NPP from minirhizotron measurements. We suggest that care should be taken when interpreting NPP results, which are likely to involve 'hidden' uncertainties from the way the estimates are constructed.

The period where productivity differences between control and eCO_2 experiments are most pronounced coincides with the previous observed increases in root width and length (Fig. 4), and not with the earlier increase in root proliferation (Fig. 2). Taken together, these observations suggest a picture where eCO_2 supports faster proliferation as roots are expanding into unoccupied space, and increased productivity due to larger fine roots in a more stable state.

5. Discussion

Taken together, our results suggest that eCO_2 provides a detectable stimulation of belowground root growth in our mature temperate

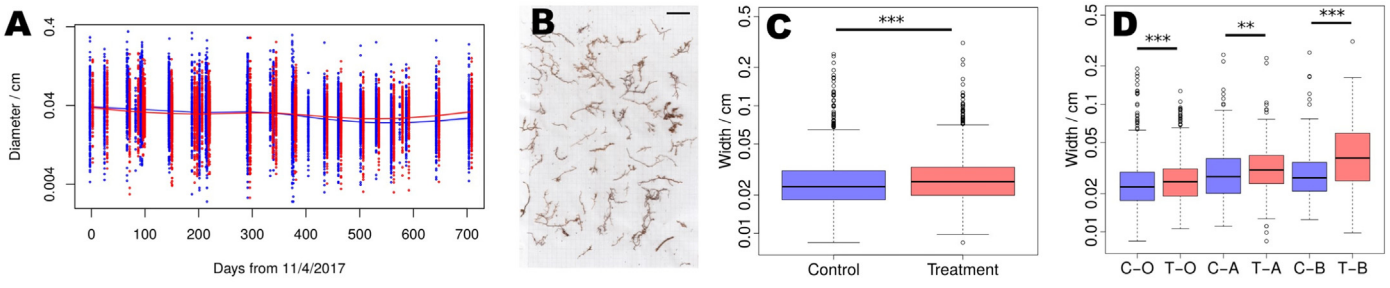

Fig. 4. Small-scale difference in root widths sampled from soil cores. (A) Fine root diameter minirhizotron observations in eCO_2 (red) and control (blue) experiments. Each datapoint is an observation from a single root segment. LOESS fits to the log-transformed data are shown with 95 % confidence intervals. (B) Example root system fragments from soil coring for individual analysis. Roots are shown on 1 cm graph paper; scale bar shows 5 cm. (C-D) Diameter of live roots taken from March 2019 soil cores under eCO_2 (red) and control (blue) conditions. (C) Logged diameter of live roots separated by treatment and control. A Mann-Whitney test shows a small but significant increase in root width under eCO_2 (1.04-fold, $p = 5 \times 10^{-9}$). (D) Logged root diameters from (C), separated by soil horizon for eCO_2 (red) and control (blue). The increase in width under eCO_2 is consistent across all 3 horizons (1.03-fold, $p = 1.5 \times 10^{-7}$; 1.02-fold, $p = 0.0031$; 1.46-fold, $p = 8.4 \times 10^{-7}$ for O, A, and B respectively).

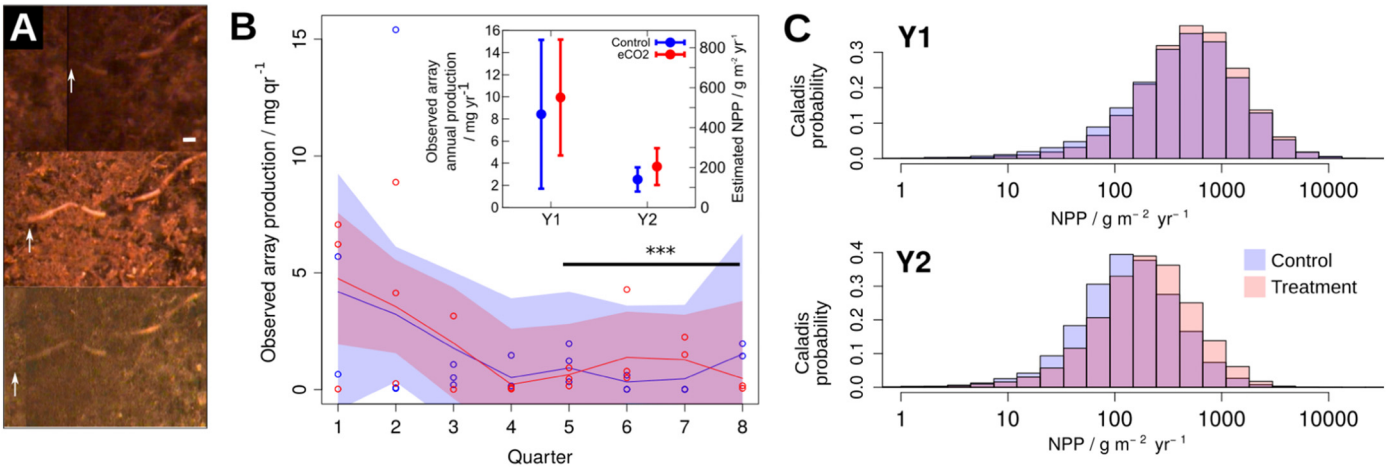

Fig. 5. Net primary productivity estimates and uncertainties. (A) Example of month-by-month root dynamics (here, elongation) for belowground NPP calculations. Arrows identify the root tip, extending over time, and the horizontal scale bar represents 1 mm. (B) Observed fine root production per plot per year quarter (i.e. 3-month period) and total across plots per year (inset) from root observations under eCO_2 (red) and ambient air (blue), with LOESS fits and 95 % confidence intervals. Dynamics in quarters 5–8 (***) display significant differences between eCO_2 and control (likelihood ratio test comparing quadratic models, $p = 2.6 \times 10^{-4}$), though see text for interpretation. Error bars in inset are s.e.m. taken across independent arrays. (C) Caladis, a calculator for uncertain quantities (Johnston et al., 2014) (see text and Methods) was used to characterise probability distributions of NPP estimates in year 1 and year 2 of our observations, reflecting the uncertainty propagated through the quantities combines to make these estimates.

deciduous woodland. We found that relative rates of fine root proliferation detectably increased under eCO_2 in the first year of treatment and also differed, to a lesser extent, in the second year. Several detectable differences were already observed in this first period – and as responses to eCO_2 are expected to manifest over longer timescales, ongoing observations are being made to further explore the time behaviour of the quantities we measure here.

Some external influences on the system's behaviour must be discussed. First, some of the earliest seasonal change may be due to a wounding response, inducing increased root production, due to the disturbance caused by the minirhizotron installation four months earlier (Johnson et al., 2001) (see Methods). However, the processes of installation and soil settling were not systematically different in control versus eCO_2 plots, suggesting that comparisons of behaviour between plot types will be informative of eCO_2 effects while controlling for these transient influences. Second, some of the reduction in biomass across the arrays in the second year of sampling may be attributed to environmental effects on the forest. The summer of 2018 was particularly dry, and the trees were recovering from a springtime infestation of winter moth (*Operophtera brumata*) caterpillars (17th May to 3rd June) (Kris Hart, Personal Communication). The insect herbivory is evident directly in canopy photography and as a decrease in canopy greenness (see Northern Arizona University phenocam image repository for Mill Haft: https://phenocam.nau.edu/webcam/roi/millhaft/DB_1000/), and the outbreak was corroborated by frass fall into litter traps and by direct capture of moth larvae by the technical team (for more details, see Roberts et al. (2022)). Again, these influences did not affect one plot type systematically more than another, and so control-eCO_2 comparisons remain informative for eCO_2 behaviour. Indeed, these influences demonstrate the importance of the control measurement set, characterising the seasonal and specific variation experienced by the system and allowing us to account for behaviour that is likely genuinely due to eCO_2.

At later stages of the experiment, other differences became clear, with increases in fine root width and length in later soil cores revealed through large-scale morphological assessment, and an increase in observed fine root production under eCO_2. This pattern of observations is compatible with a picture where eCO_2 has joint effects, which the different years of our observations illustrate: during expansion, when roots are growing into new space, eCO_2 increases the proliferation rate of fine roots, and in more stable root layouts, eCO_2 supports the expansion of existing roots. Further observations from the system will be used in future to test this picture, and specifically the hypothesis that existing, established roots will expand at higher rates under eCO_2.

The largest effect we observe is the increase in peak observed root productivity in the second year, suggesting that the increase in root size due to eCO_2 fertilisation may be the dominant effect in our system. Considering means alone, eCO_2 was responsible for a 46 % increase in annual estimated belowground NPP, reflecting a potentially substantial influence on the belowground system – as found in studies of other systems (Norby et al., 2004; Iversen, 2010; Iversen et al., 2008; Pritchard et al., 2008). However, the dynamics leading to these results are nuanced and the values are subject to uncertainty, as described above, and hence propagating such values into other models and analyses must be done with caution and this uncertainty explicitly tracked.

As with any experimental approaches aimed at this challenging system, the methods we use require some scrutiny. For comparison, we first note that our estimates of NPP are broadly similar to those from similar studies (Terrer et al., 2019; Norby and Zak, 2011) (which fall, for example, around 100–200 g dw m^{-2} yr^{-1} (Pritchard et al., 2008); 100–400 g C m^{-2} yr^{-1} (Norby et al., 2004), and 40–500 g C m^{-2} yr^{-1} in Wytham woods, a more similar ecosystem (Fenn et al., 2015)). The increase of fine root productivity under 150 ppm eCO_2 that we observe (1.17- to 1.45-fold) agrees well with that observed in a recent study characterising the carbon budget of a mature eucalyptus forest (1.22-fold) (Jiang et al., 2020) and more broadly with estimates that eCO_2 may drive a 12 % (i.e. 1.12-fold) increase in plant biomass (Terrer et al., 2019). Observation of year-to-year variation in this behaviour is not inconsistent with other studies (Iversen et al., 2008) (which often show a slowing of NPP enhancement effects over time (Norby and Zak, 2011)) and will be further characterised in ongoing study of this system. We note here that the conversion from estimates of dry weight biomass (g dw m^{-2} yr^{-1}) to carbon biomass (g C m^{-2} yr^{-1}) includes another uncertainty, the proportional contribution of carbon to root dry mass. We do not focus on this conversion here but a convenient heuristic is that dry mass is around 50 % carbon (Petrokofsky et al., 2012).

One source of variability in our study is the diversity of plant life in our research site (Körner, 2005). We do not attempt to classify roots based on phylogenetics, instead relying on our sampling across physical positions, different arrays, and comparison to control arrays embedded in the ecosystem, to mitigate against any systematic bias towards particular species. This is supported by the consistent trends we observe through several different modes of observation, and means that our results should be viewed as ecosystem-wide readouts rather than species-specific responses.

To conclude, we believe that our multi-faceted approach, using large volumes of diverse data and tracking uncertainty throughout scaling calculations, is a powerful way to address challenging questions about hard-toobserve ecosystem responses. The use of stochastic modelling rather than purely data-driven analysis increases our approach's power to detect mechanistic differences, and we believe our consideration of the (large) uncertainties involved in belowground observation has helped increase the interpretability of our findings by underlining the necessary caution required (Johnston et al., 2014). We hope that these approaches help inform the quantitative interpretation of past and future experiments on this globally important topic.

CRediT authorship contribution statement

Clare Ziegler – Data curation, Formal analysis, Investigation, Methodology, Resources, Software, Validation, Visualisation, Writing – original draft; Writing – review & editing

Aleksandra Kulawska – Data curation, Formal analysis, Investigation, Visualisation, Writing – review & editing

Angeliki Kourmouli – Data curation, Formal analysis, Investigation, Visualisation, Writing – review & editing

Liz Hamilton – Resources, Writing – review & editing

Zongbo Shi – Resources, Writing – review & editing

A. Rob MacKenzie – Conceptualization, Funding acquisition, Project administration, Resources, Supervision, Writing – review & editing

Rosemary J. Dyson – Conceptualization, Resources, Supervision, Writing – review & editing

Iain G. Johnston – Conceptualization, Data curation, Formal analysis, Funding acquisition, Investigation, Methodology, Project administration, Resources, Software, Supervision, Validation, Visualization, Writing – original draft, Writing – review & editing

Data availability

All raw data (and analysis code) are available at https://github.com/stochasticbiology/elevated-co2

Declaration of competing interest

The authors declare that no competing interests exist.

Acknowledgements

All authors acknowledge support from the Birmingham Institute of Forest Research, and from the workshop at the School of Biosciences, University of Birmingham. IGJ acknowledges support from a Birmingham Fellowship for the University of Birmingham and Turing Fellowship from the Alan Turing Institute. BIFoR FACE is supported by the JABBS foundation and the University of Birmingham. Aleks K is supported by the Natural Environment Research Council through a CENTA studentship. This project has been supported by QUINTUS, NERC Large Grant NE/S015833/1. The authors gratefully acknowledge advice and critique received from Prof Rich Norby throughout the study.

Appendix A. Supplementary data

Supplementary data to this article, including supplementary images and mathematical derivations, can be found online at https://doi.org/10.1016/j.scitotenv.2022.158661.

References

Allen, A.S., Andrews, J.A., Finzi, A.C., Matamala, R., Richter, D.D., Schlesinger, W.H., 2000. Effects of free-air CO2 enrichment (FACE) on belowground processes in a Pinus taeda forest. Ecol. Appl. 10 (2), 437–448.

Bader, Martin, Hiltbrunner, Erika, Korner, Christian, 2009. Fine root responses of mature deciduous forest trees¨ to free air carbon dioxide enrichment (FACE). Funct. Ecol. 23 (5), 913–921.

Bradley, Kate L., Pregitzer, Kurt S., 2007. Ecosystem assembly and terrestrial carbon balance under elevated CO2. Trends Ecol. Evol. 22 (10), 538–547.

Cavagnaro, T.R., Gleadow, R.M., Miller, R.E., 2011. Plant nutrient acquisition and utilisation in a high carbon dioxide world. Funct. Plant Biol. 38 (2), 87–96.

Cheng, W., Dan, L., Deng, X., et al., 2022. Global monthly gridded atmospheric carbon dioxide concentrations under the historical and future scenarios. Sci. Data 9, 83. https://doi.org/10.1038/s41597-022-01196-7).

Ciais, Philippe, Sabine, Christopher, 2013. Carbon and other biogeochemical cycles, chapter 6. Climate Change 2013: The Physical Science Basis (IPCC AR5), pp. 465–570.

Cleland, Elsa E., Chuine, Isabelle, Menzel, Annette, Mooney, Harold A., Schwartz, Mark D., 2007. Shifting plant phenology in response to global change. Trends Ecol. Evol. 22 (7), 357–365.

Clemmensen, K.E., Bahr, Adam, Ovaskainen, O., Dahlberg, A., Ekblad, Alf, Wallander, Hakan, Stenlid, J., Finlay, R.D., Wardle, D.A., Lindahl, B.D., 2013. Roots and associated fungi drive long-term carbon sequestration in boreal forest. Science 339 (6127), 1615–1618.

Duursma, Remko A., Gimeno, Teresa E., Boer, Matthias M., Crous, Kristine Y., Tjoelker, Mark G., Ellsworth, David S., 2016. Canopy leaf area of a mature evergreen eucalyptus woodland does not respond to elevated atmospheric [CO2] but tracks water availability. Glob. Chang. Biol. 22 (4), 1666–1676.

Edwards, Everard J., McCaffery, Stephanie, Evans, John R., 2006. Phosphorus availability and elevated CO2 affect biological nitrogen fixation and nutrient fluxes in a clover-dominated sward. New Phytol. 169 (1), 157–167.

Ellsworth, David S., Anderson, Ian C., Crous, Kristine Y., Cooke, Julia, Drake, John E., Gherlenda, Andrew N., Gimeno, Teresa E., Macdonald, Catriona A., Medlyn, Belinda E., Powell, Jeff R., et al., 2017. Elevated CO2 does not increase eucalypt forest productivity on a low-phosphorus soil. NatureClimate Change 7 (4), 279.

Felipe-Lucia, Maria R., Soliveres, Santiago, Penone, Caterina, Manning, Peter, van der Plas, Fons, Boch, Steffen, Prati, Daniel, Ammer, Christian, Schall, Peter, Gossner, Martin M., et al., 2018. Multiple forest attributes underpin the supply of multiple ecosystem services. Nature Communications 9 (1), 4839.

Fenn, K., Malhi, Y., Morecroft, M., Lloyd, C., Thomas, M., 2015. The carbon cycle of a maritime ancient temperate broadleaved woodland at seasonal and annual scales. Ecosystems 18 (1), 1–15.

Ferguson, J.C., Smucker, A.J.M., 1989. Modifications of the minirhizotron video camera system for measuring spatial and temporal root dynamics. Soil Sci. Soc. Am. J. 53 (5), 1601–1605.

Fernando, Nimesha, Panozzo, Joe, Tausz, Michael, Norton, Robert M., Neumann, Nathan, Fitzgerald, Glenn J., Seneweera, Saman, 2014. Elevated CO2 alters grain quality of two bread wheat cultivars grown under different environmental conditions. Agriculture, Ecosystems & Environment 185, 24–33.

Finzi, Adrien C., Abramoff, Rose Z., Spiller, Kimberly S., Brzostek, Edward R., Darby, Bridget A., Kramer, Mark A., Phillips, Richard P., 2015. Rhizosphere processes are quantitatively important components of terrestrial carbon and nutrient cycles. Glob. Chang. Biol. 21 (5), 2082–2094.

Gardner, A., Ellsworth, D.S., Crous, K.Y., Pritchard, J., MacKenzie, A.R., 2022. Is photosynthetic enhancement sustained through three years of elevated CO2 exposure in 175-year-old Quercus robur? Tree Physiology 42 (1), 130–144.

Gill, Richard A., Jackson, Robert B., 2000. Global patterns of root turnover for terrestrial ecosystems. New Phytol. 147 (1), 13–31.

Hart, Kris M., Curioni, Giulio, Blaen, Phillip, Harper, Nicholas J., Miles, Peter, Lewin, Keith F., Nagy, John, Bannister, Edward J., Cai, Xiaoming M., Thomas, Rick M., et al., 2019. Characteristics of free air carbon dioxide enrichment of a northern temperate mature forest. Global change biology 26, 1023–1037.

Hendrey, George R., Ellsworth, David S., Lewin, Keith F., Nagy, JohN, 1999. A free-air enrichment system for exposing tall forest vegetation to elevated atmospheric CO2. Glob. Chang. Biol. 5 (3), 293–309.

Iuss Working Group Wrb, 2015. World reference base for soil resources 2014. Update2015: International Soil Classification System for Naming Soils and CreatingLegends for Soil Maps.

Iversen, Colleen M., 2010. Digging deeper: fine-root responses to rising atmospheric CO2 concentration in forested ecosystems. New Phytol. 186 (2), 346–357.

Iversen, Colleen M., Ledford, Joanne, Norby, Richard J., 2008. CO2 enrichment increases carbon and nitrogen input from fine roots in a deciduous forest. New Phytol. 179 (3), 837–847.

Jackson, R.B., Mooney, H.A., Schulze, E.-D., 1997. A global budget for fine root biomass, surface area, and nutrient contents. Proc. Natl. Acad. Sci. 94 (14), 7362–7366.

Jiang, Mingkai, Medlyn, Belinda E., Drake, John E., Duursma, Remko A., Anderson, Ian C., Barton, Craig V.M., Boer, Matthias M., Carrillo, Yolima, Castaneda-Gõmez, Laura, Collins, Luke, et al., 2020. The fate of carbon in a mature´ forest under carbon dioxide enrichment. Nature 580 (7802), 227–231.

Johnson, M.G., Meyer, P.F., 1998. Mechanical advancing handle that simplifies minirhizotron camera registration and image collection. J. Environ. Qual. 27 (3), 710–714.

Johnson, M.G., Tingey, D.T., Phillips, D.L., Storm, M.J., 2001. Advancing fine root research with minirhizotrons. Environ. Exp. Bot. 45 (3), 263–289.

Johnson, D.W., Cheng, W., Joslin, J.D., Norby, R.J., Edwards, N.T., Todd, D.E., 2004. Effects of elevated CO2 on nutrient cycling in a sweetgum plantation. Biogeochemistry 69 (3), 379–403.

Johnston, Iain G., Jones, Nick S., 2015. Closed-form stochastic solutions for non-equilibrium dynamics and inheritance of cellular components over many cell divisions. Proceedings of the Royal Society A: Mathematical, Physical and Engineering Sciences 471 (2180), 20150050.

Johnston, Iain G., Rickett, Benjamin C., Jones, Nick S., 2014. Explicit tracking of uncertainty increases the power of quantitative rule-of-thumb reasoning in cell biology. Biophys. J. 107 (11), 2612–2617.

Körner, C., 2005. An introduction to the functional diversity of temperate forest trees. Forest Diversity and Function. Springer, Berlin, Heidelberg, pp. 13–37.

Kris Hart. Personal Communication.n.d.
Lapola, D.M., Norby, R.J., 2014. Amazon-FACE:Assessing The Effects Of Increased Atmospheric CO2 on the Ecology and Resilienceof the Amazon Forest–Science Plan and Implementation Strategy. Ministry of Science, Technology and Science, Brasilia, Brazil.
Lobet, Guillaume, Pages, Löic, Draye, Xavier, 2011. A novel image-analysis toolbox enabling quantitative analysis` of root system architecture. Plant Physiology 157 (1), 29–39.
MacKenzie, A.R., Krause, S., Hart, K.M., Thomas, R.M., Blaen, P.J., Hamilton, R.L., Curioni, G., Quick, S.E., Kourmouli, A., Hannah, D.M., et al., 2021. BIFoR FACE: water-soil-vegetation-atmosphere data from a temperate deciduous forest catchment, including under elevated CO2. Hydrol. Process. 35, e14096.
MacKenzie, A.R., Krause, S., Hart, K.M., Thomas, R.M., Blaen, P.J., Hamilton, R.L., Curioni, G., Quick, S.E., Kourmouli, A., Hannah, D.M., Comer-Warner, S.A., Brekenfeld, N., Ullah, S., Press, M.C., 2021. BIFoR FACE: water-soil-vegetation-atmosphere data from a temperate deciduous forest catchment, including under elevated CO2. Hydrol. Process. 35, e14096. https://doi.org/10.1002/hyp.14096.
Madhu, M., Hatfield, J.L., 2013. Dynamics of plant root growth under increased atmospheric carbon dioxide. Agron. J. 105 (3), 657–669.
Majdi, Hooshang, 1996. Root sampling methods-applications and limitations of the minirhizotron technique. Plant Soil 185 (2), 255–258.
Marklein, Alison R., Houlton, Benjamin Z., 2012. Nitrogen inputs accelerate phosphorus cycling rates across a wide variety of terrestrial ecosystems. New Phytol. 193 (3), 696–704.
Masson-Delmotte, V., Zhai, P., Portner, H.-O., Roberts, D., Skea, J., Shukla, P.R., Pirani, A., Moufouma-Okia, W., Pean, C., Pidcock, R., Connors, S., Matthews, J.B.R., Chen, Y., Zhou, X., Gomis, M.I., Lonnoy, E., Maycock, T., Tignor, M., Waterfield, T., 2018. GlobalWarming of 1.5° C. An IPCC Special Report on the Impacts of Global Warming of1.5° C Above Pre-industrial Levels and Related Global Greenhouse Gas EmissionPathways, in the Context of Strengthening the Global Response to the Threat of ClimateChange, Sustainable Development, and Efforts to Eradicate Poverty. World Meteorological Organization, Geneva, Switzerland.
Matamala, Roser, Gonzalez-Meler, Miquel A., Jastrow, Julie D., Norby, Richard J., Schlesinger, William H., 2003. Impacts of fine root turnover on forest NPP and soil C sequestration potential. Science 302 (5649), 1385–1387.
Medlyn, Belinda E., Zaehle, Sonke, De Kauwe, Martin G., Walker, Anthony P., Dietze, Michael C., Hickler, Thomas, Jain, Atul K., Luo, Yiqi, Parton, William, et al., Hanson, Paul J., 2015. Using ecosystem experiments to improve vegetation models. Nature Climate Change 5 (6), 528.
Myers, Samuel S., Zanobetti, Antonella, Kloog, Itai, Huybers, Peter, Leakey, Andrew D.B., Bloom, Arnold J., Carlisle, Eli, Dietterich, Lee H., Fitzgerald, Glenn, Hasegawa, Toshihiro, et al., 2014. Increasing CO2 threatens human nutrition. Nature 510 (7503), 139–142.
Norby, R.J., Zak, D.R., 2011. Ecological lessons from free-air CO2 enrichment (FACE) experiments. Annu. Rev. Ecol. Evol. Syst. 42 (1), 181–203.
Norby, Richard J., Hanson, Paul J., O'Neill, Elizabeth G., Tschaplinski, Tim J., Weltzin, Jake F., Hansen, Randi A., Cheng, Weixin, Wullschleger, Stan D., Gunderson, Carla A., Edwards, Nelson T., et al., 2002. Net primary productivity of a CO2-enriched deciduous forest and the implications for carbon storage. Ecological Applications 12 (5), 1261–1266.
Norby, Richard J., Ledford, Joanne, Reilly, Carolyn D., Miller, Nicole E., O'Neill, Elizabeth G., 2004. Fine-root production dominates response of a deciduous forest to atmospheric CO2 enrichment. Proceedings of the national Academy of Sciences 101 (26), 9689–9693.
Norby, Richard J., Warren, Jeffrey M., Iversen, Colleen M., Medlyn, Belinda E., McMurtrie, Ross E., 2010. CO2 enhancement of forest productivity constrained by limited nitrogen availability. Proceedings of the National Academy of Sciences 107 (45), 19368–19373.
Norby, Richard J., De Kauwe, Martin G., Domingues, Tomas F., Duursma, Remko A., Ellsworth, David S., Goll, Daniel S., Lapola, David M., Luus, Kristina A., Rob MacKenzie, A., Medlyn, Belinda E., et al., 2016. Model–data synthesis for the next generation of forest free-air CO2 enrichment (FACE) experiments. New Phytol. 209 (1), 17–28.
Norton, Rob, Mollah, Mahabubur, Fitzgerald, Glenn, McNeil, David, 2008. The australian grains free air carbon dioxide enrichment (AGFACE) experiment–specifications and scope. Proceedings of the 14th Australian Agronomy Conference.
Nowak, Robert S., Ellsworth, David S., Smith, Stanley D., 2004. Functional responses of plants to elevated atmospheric CO2–do photosynthetic and productivity data from FACE experiments support early predictions? New Phytol. 162 (2), 253–280.
Oak Ridge National Laboratory n.d.Global List of FACE Experiments, 19/05/17 12:43. https://facedata.ornl.gov/global face.html#UrbanaPlus.
Pan, Yude, Birdsey, Richard A., Fang, Jingyun, Houghton, Richard, Kauppi, Pekka E., Kurz, Werner A., Phillips, Oliver L., Shvidenko, Anatoly, Lewis, Simon L., Canadell, Josep G., et al., 2011. A large and persistent carbon sink in the world's forests. Science 333 (6045), 988–993.
Pepin, Steeve, Korner, Christian, 2002. Web-FACE: a new canopy free-air CO¨ 2 enrichment system for tall trees in mature forests. Oecologia 133 (1), 1–9.
Petrokofsky, Gillian, Kanamaru, Hideki, Goetz, Scott J., Joosten, Hans, Holmgren, Peter, Menton, Mary C.S., Pullin, Andrew S., Wattenbach, Martin, Achard, Frederic, Lehtonen, Aleksi, 2012. Comparison of methods for measuring and assessing carbon stocks and carbon stock changes in terrestrial carbon pools. How do the accuracy and precision of current methods compare? A systematic review protocol. Environmental Evidence 1 (1), 6.
Pritchard, Seth G., Strand, Allan E., Luke McCormack, M., Davis, Micheal A., Finzi, Adrien C., Jackson, Robert B., Matamala, Roser, Rogers, Hugo H., Oren, R.A.M., 2008. Fine root dynamics in a loblolly pine forest are influenced by free-air-CO2-enrichment: a six-year-minirhizotron study. Glob. Chang. Biol. 14 (3), 588–602.
Pugh, T.A.M., Muller, C., Arneth, Almuth, Haverd, Vanessa, Smith, Benjamin, 2016. Key knowledge and data gaps¨ in modelling the influence of CO2 concentration on the terrestrial carbon sink. J. Plant Physiol. 203, 3–15.
Quere, C., Andrew, Robbie M., Friedlingstein, Pierre, Sitch, Stephen, Pongratz, Julia, Manning, Andrew C., Korsbakken, Jan Ivar, Peters, Glen P., Canadell, Josep G., Jackson, Robert B., et al., 2018. Global carbon budget 2017. Earth Syst. Sci. Data 10 (1), 405–448.
Reich, P.B., Hobbie, S.E., Lee, T.D., 2014. Plant growth enhancement by elevated CO2 eliminated by joint water and nitrogen limitation. Nature Geoscience 7 (12), 920–924.
Roberts, A.J., Crowley, L.M., Sadler, J.P., Nguyen, T.T.T., Gardner, A.M., Hayward, S.A.L., Metcalfe, D.B., 2022. Effects of elevated atmospheric CO2 concentration on insect herbivory and nutrient fluxes in a mature temperate Forest. Forests 13, 998.
Rogers, Hugo H., Runion, G.Brett, Prior, A., 1999. Response of plants to elevated atmospheric CO2: root growth, mineral. Carbon Dioxide and Environmental Stress, p. 215.
Samson, Benjamin K., Sinclair, Thomas R., 1994. Soil core and minirhizotron comparison for the determination of root length density. Plant Soil 161 (2), 225–232.
Santantonio, D., Hermann, R.K., 1985. Standing crop, production, and turnover of fine roots on dry, moderate, and wet sites of mature Douglas-fir in western Oregon. Annales des Sciences Forestieres. 42, pp. 113–142 EDP Sciences.
Schindelin, Johannes, Arganda-Carreras, Ignacio, Frise, Erwin, Kaynig, Verena, Longair, Mark, Pietzsch, Tobias, Preibisch, Stephan, Rueden, Curtis, Saalfeld, Stephan, Schmid, Benjamin, et al., 2012. Fiji: an open-source platform for biological-image analysis. Nat. Methods 9 (7), 676.
Schneider, Caroline A., Rasband, Wayne S., Eliceiri, Kevin W., 2012. NIH Image to ImageJ: 25 years of image analysis. Nature Methods 9 (7), 671.
Taylor, H.M., Upchurch, D.R., McMichael, B.L., 1990. Applications and limitations of rhizotrons and minirhizotrons for root studies. Plant Soil 129 (1), 29–35.
Taylor, Benton N., Beidler, Katilyn V., Strand, Allan E., Pritchard, Seth G., 2014. Improved scaling of minirhizotron data using an empirically-derived depth of field and correcting for the underestimation of root diameters. Plant Soil 374 (1–2), 941–948.
Team, R.Core, 2015. R: A Language and Environment for Statistical Computing. R Foundation for Statistical Computing, Vienna, Austria.
Terrer, C., Jackson, R.B., Prentice, I.C., Keenan, T.F., Kaiser, C., Vicca, S., Fisher, J.B., Reich, P.B., Stocker, B.D., Hungate, B.A., Peñuelas, J., 2019. Nitrogen and phosphorus constrain the CO2 fertilization of global plant biomass. Nat. Clim. Chang. 9 (9), 684–689.
Thilakarathne, Chamindathee L., Tausz-Posch, Sabine, Cane, Karen, Norton, Robert M., Fitzgerald, Glenn J., Tausz, Michael, Seneweera, Saman, 2015. Intraspecific variation in leaf growth of wheat (Triticum aestivum) under Australian Grain Free Air CO2 Enrichment (AGFACE): is it regulated through carbon and/or nitrogen supply? Functional Plant Biology 42 (3), 299–308.
Tierney, Geraldine L., Fahey, Timothy J., 2001. Evaluating minirhizotron estimates of fine root longevity and production in the forest floor of a temperate broadleaf forest. Plant Soil 229 (2), 167–176.
U.S. Department of Energy, 2020. U.S. Department of Energy Free-Air CO2 Enrichment Experiments: FACE Results, Lessons, and Legacy, DOE/SC–0202.
Zaehle, Sonke, Medlyn, Belinda E., De Kauwe, Martin G., Walker, Anthony P., Dietze, Michael C., Hickler, Thomas, Luo, Yiqi, Wang, Ying-Ping, El-Masri, Bassil, Thornton, Peter, et al., 2014. Evaluation of 11 terrestrial carbon–nitrogen cycle models against observations from two temperate free-Air CO2 enrichment studies. New Phytologist 202 (3), 803–822.